ChemPubSoc Europe

DOI: 10.1002/ejic.201801221

EurJIC European Journal of Inorganic Chemistry

Full Paper

Cobalt-Catalyzed Hydrosilylation

Cobalt(II) and (I) Complexes of Diphosphine-Ketone Ligands: Catalytic Activity in Hydrosilylation Reactions

Dide G. A. Verhoeven,[a] Joost Kwakernaak,[a] Maxime A. C. van Wiggen,[a] Martin Lutz,[b] and Marc-Etienne Moret*[a]

Abstract: The hydrosilylation of unsaturated compounds homogeneously catalyzed by cobalt complexes has gained considerable attention in the last years, aiming at substituting precious metal-based catalysts. In this study, the catalytic activity of well-characterized Co^{II} and Co^{I} complexes of the ^{pTol}dpbp ligand is demonstrated in the hydrosilylation of 1-octene with phenylsilane. The Co^{I} complex is the better precatalyst for the mentioned reaction under mild conditions, at 1 mol-% catalyst, 1 h, room temperature, and without solvent, yielding 84 % of octylphenylsilane. Investigation of the substrate scope shows lower performance of the catalyst in styrene hydrosilylation, but excellent results with allylbenzene (84 %) and acetophenone (> 99 %). This catalytic study contributes to the field of cobalt-catalyzed hydrosilylation reactions and shows the first example of catalysis employing the dpbp ligand in combination with a base metal.

Introduction

The hydrosilylation of unsaturated compounds catalyzed by cobalt complexes has received significant attention in recent years.[1–4] This reaction is highly important in the silicon industry as it is used in the synthesis of silicon polymers, oils and resins, as well as in the production of organosilicon reagents for fine chemicals.[5] Generally, extremely active and selective Pt-based homogeneous catalysts, such as Speier's or Karstedt's catalysts,[6–8] are used but the ongoing quest for more sustainable processes leads to interest in employing base metals iron,[9–11] cobalt and nickel.[12–15] While hydrosilylation catalyzed by the low-valent Co^0 complex $Co_2(CO)_8$ was reported as early as 1965 by Chalk and Harrod,[16–19] the number of cobalt catalysts increased explosively in recent years.

The scope for the unsaturated substrate is versatile, including alkene,[1,11,20–28] alkyne,[29–33] carbonyl[34,35] and carboxylic derivative[36] groups. Additionally, a number of different silanes can be used: much research is performed with phenylsilane, and other silanes such as diphenylsilane,[24] alkyl silanes,[20] and alkoxy silanes[24,37] can be employed as well. Prominent examples for hydrosilylation of alkenes with phenylsilane are the β-diketiminate cobalt complexes reported by Holland,[22] the phosphine-iminopyridine cobalt complexes used by Huang[11] and the bis(carbene)cobalt-dinitrogen complex by Fout (Figure 1).[24] Ge and co-workers developed efficient cobalt-based systems for the hydrosilylation of dienes, employing an in situ generated catalyst from commercially available $Co(acac)_2$ in combination with common diphosphine [e.g. xanthphos, binap, 1,2-(diphenylphosphine)ethane] or trinitrogen (e.g. substituted pyridinediimine) ligands.[32,38] The first step in the catalytic cycle of hydrosilylation reactions is commonly the oxidative addition of the silane substrate, forming metal-hydrides.[16] To assist this two-electron step on cobalt – a first-row transition metal with the tendency to undergo one-electron steps – the incorporation of cooperative ligands is of interest.[34,39,40] An instructive example was recently reported by the group of Peters, wherein diphosphine-borane cobalt-dinitrogen complexes cooperatively activate the silane substrate in the catalytic hydrosilylation of carbonyl compounds (Figure 1).[34]

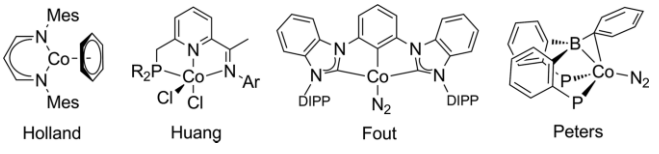

Figure 1. Examples of cobalt catalysts for hydrosilylation reactions. P in rightmost structure: P*i*Pr$_2$.

We previously described the coordination of the diphosphine ketone ligand ^{Ph}dpbp (**1^{Ph}**, Figure 2) to base metals Fe, Co, Ni and Cu.[39,41] Especially, exploration of the cobalt complexes in hydrosilylation reactions is of interest given the recent success in the field. Cobalt complexes (^{Ph}dpbp)$CoCl_2$ (**2^{Ph}**) and (^{Ph}dpbp)CoCl (**3^{Ph}**) illustrate the particular hemilabile behavior of the ketone moiety upon changing the oxidation state from

[a] *Organic Chemistry & Catalysis, Debye Institute for Nanomaterials Science, Faculty of Science, Utrecht University, Universiteitsweg 99, 3584 CG, Utrecht, The Netherlands*
E-mail: M.Moret@uu.nl
https://www.uu.nl/en/research/organic-chemistry-catalysis
[b] *Crystal and Structural Chemistry, Bijvoet Center for Biomolecular Research, Faculty of Science, Utrecht University, Padualaan 8, 3584 CH, Utrecht, The Netherlands*
Supporting information and ORCID(s) from the author(s) for this article are available on the WWW under https://doi.org/10.1002/ejic.201801221.

Co^{II} to Co^{I}, resulting in an η^2(C,O)-coordination in the latter complex (Figure 2).[39,42] The adaptivity of the ligand in combination with the accessibility of low oxidation state such as Co^{I} prompted us to evaluate the activity of these complexes for hydrosilylation. Herein, the catalytic activity of these Co^{II} and Co^{I} complexes is described. The diphosphine ketone ligand $^{p\text{Tol}}$dpbp is employed, equipped with bis(*p*-tolylphosphino) functionalities to improve solubility of the complexes during reactions with respect to the previously reported diphenylphosphino analogues.

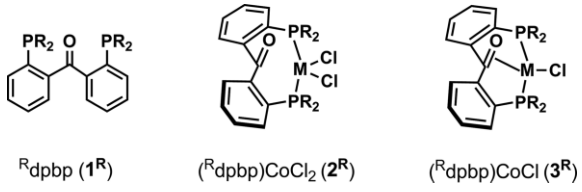

^{R}dpbp (**1^{R}**) (^{R}dpbp)$CoCl_2$ (**2^{R}**) (^{R}dpbp)CoCl (**3^{R}**)

Figure 2. Structures of ^{R}dpbp (left), (^{R}dpbp)$CoCl_2$ (middle), and (^{R}dpbp)CoCl (right). **1^{Ph}**, **2^{Ph}**, **3^{Ph}**: R = Ph; **1$^{p\text{Tol}}$**, **2$^{p\text{Tol}}$**, **3$^{p\text{Tol}}$**: R = *p*-tolyl.

Results and Discussion

Synthesis of Cobalt Complexes

The synthesis of Co^{I} complex (^{Ph}dpbp)CoCl (**3^{Ph}**) was described previously.[39] An initial experiment with **3^{Ph}** in the hydrosilylation reaction of 1-octene with phenylsilane showed promising results: applying a high catalyst loading of 10 mol-% in C_6D_6 in a Young-type NMR tube resulted in full conversion of the substrates and formation of octylphenylsilane as the major product in 30 min. However, the low solubility of the precatalyst resulted in a turbid mixture during catalysis. To improve solubility, the phenyl groups of ^{Ph}dpbp were replaced by *p*-tolyl groups, with the additional benefit of providing a convenient handle for NMR analysis of the complex. The ligand $^{p\text{Tol}}$dpbp (**1$^{p\text{Tol}}$**) was synthesized in two steps similarly to its phenyl substituted analogue, via first a Pd-catalyzed cross coupling reaction to yield the *o*-bromo-substituted phenyldi-*p*-tolylphosphine precursor which was subsequently lithiated and used in a double nucleophilic substitution reaction on dimethylcarbamylchloride, resulting in the diphosphine-ketone ligand (Scheme 1).[39,41]

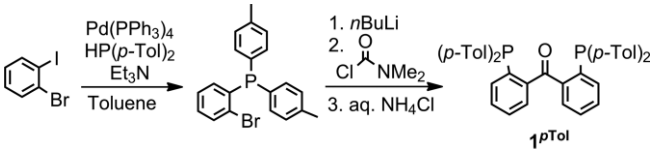

Scheme 1. Synthesis of **1$^{p\text{Tol}}$**.

A Co^{II} complex was formed by addition of $^{p\text{Tol}}$dpbp to $CoCl_2$ in CH_2Cl_2 resulting in ($^{p\text{Tol}}$dpbp)$CoCl_2$ (**2$^{p\text{Tol}}$**) after workup. The ^{1}H NMR spectrum shows the formation of a species with signals from 18 to –2 ppm, and no peak was observed in the corresponding ^{31}P NMR spectrum, indicating the formation of a paramagnetic species. A distorted tetrahedral cobalt center is observed in the crystal structure of **2$^{p\text{Tol}}$** with the two phosphine tethers of the ligand coordinated to the metal center, next to two chloride ligands (Figure 3, top). The P–Co–P angle is 115.734(16)°, akin to **2^{Ph}** (Table 1).[39] The ketone moiety of the ligand backbone has a C=O bond length of 1.2262(19) Å and Co–C and Co–O distances of 3.3599(15) Å and 3.0474(13) Å, respectively, and is not coordinated to cobalt. Reduction of the Co^{II} complex with sodium naphthalide in THF results in the Co^{I} complex ($^{p\text{Tol}}$dpbp)CoCl (**3$^{p\text{Tol}}$**) after precipitation from the mixture with hexanes, followed by extraction of the product with THF and evaporation of the solvents. ^{1}H NMR analysis indicates once more the formation of a paramagnetic species with signals from 33 to –17 ppm. Distinctive signals for the *p*-tolyl methyl groups are present at 9.24 and 17.67 ppm, identified by integration and comparison to **3^{Ph}**, and the magnetic moment of the complex as measured by Evans method (μ_{eff} = 2.8) indicates a spin state of S = 1. Whereas the phenyl-substituted analogue **3^{Ph}** was reluctant to crystallization, slow vapor diffusion of toluene/hexanes with **3$^{p\text{Tol}}$** resulted in single crystals suitable for X-ray diffraction. As the crystal structure of **3$^{p\text{Tol}}$** was reported earlier,[39] it is discussed here for comparison with that of **2$^{p\text{Tol}}$**. It reveals a tetrahedral geometry around Co with $^{p\text{Tol}}$dpbp bound in a κ^4(P,P,C,O)-fashion, including an η^2(C,O)-coordination of the ketone, and coordination of both phosphine groups (Figure 3, bottom). Next to this, a chloride is bound to cobalt. The C–O bond is elongated due to π-backdonation in the π^* antibonding orbital of the ketone moiety from 1.2262(19) Å in **2$^{p\text{Tol}}$** to 1.307(6) Å in **3$^{p\text{Tol}}$**. This is similar to the elongation as found in the Fe^{I} and Ni^{I} complexes [C–O bond length for Fe^{II}: 1.218(3), Fe^{I}: 1.3296(14), Ni^{II}: 1.2288(16) and Ni^{I}: 1.310(2) Å].[39]

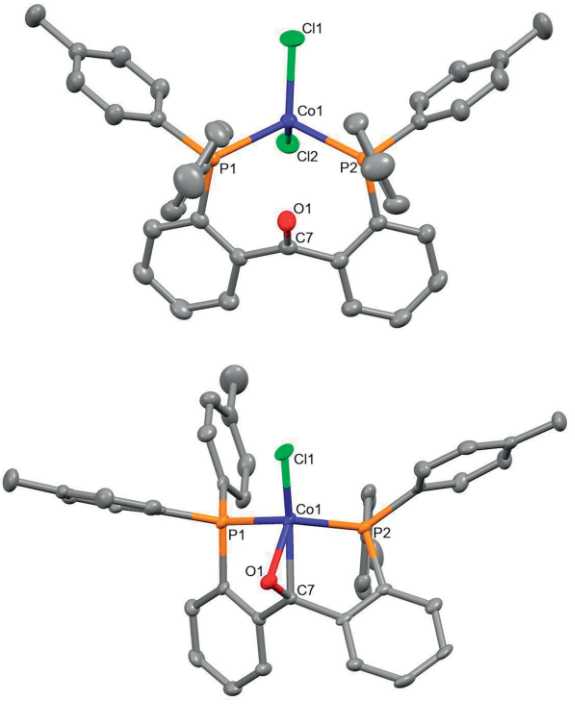

Figure 3. X-ray crystal structures of **2$^{p\text{Tol}}$** (top) and **3$^{p\text{Tol}}$** (bottom).[39] Hydrogen atoms are omitted for clarity and the ellipsoids are shown at 50 % probability level. In **2$^{p\text{Tol}}$**: the co-crystallized THF molecule was omitted for clarity.

Table 1. Crystal structure comparison of the cobalt complexes. Selected distances [Å] and angles [°].

	Co–O1	Co–C7	C7–O1	P1–Co–P2	Dihedral angle[a]	IR C=O cm^{-1}
2^{Ph} [39]	2.9255(13)	3.2896(18)	1.227(2)	116.676(18)	36.16(9)	1647
2^{pTol}	3.0474(13)	3.3599(15)	1.2262(19)	115.734(16)	34.03(8)	1663
3^{pTol} [39]	1.947(3)	2.071(5)	1.307(6)	109.62(6)	64.2(2)	≈ 1300

[a] The dihedral angle is calculated between the two phenyl rings connected to the carbonyl group.

Hydrosilylation Reactions

The reactivity of Co^{I} complex **3^{pTol}** with phenylsilane was explored. Addition of 3 eq of $PhSiH_3$ to **3^{pTol}** in C_6D_6 lead to an exothermic reaction, resulting in a mixture of species. The ^1H NMR spectrum shows a diamagnetic spectrum containing three broad signals around –12 ppm, of which one exhibits apparent triplet multiplicity, consistent with the presence of one or more diamagnetic Co^{I}-hydride species (supporting info, Figure S14, S15).[43,44] Attempts to perform further analyses were unsuccessful due to the high reactivity of the obtained Co–H species, therefore the structure has not been elucidated. Nevertheless, the high reactivity prompted for further investigation on catalytic hydrosilylation by **3^{pTol}**.

Pre-catalyst **3^{pTol}** is active in the hydrosilylation reaction of 1-octene with phenylsilane, resulting in 98 % conversion of both substrates with 84 % octylphenylsilane as product (Table 2, Entry 1).[45] Initial optimization lead to the following standard conditions: 1 mol-% **3^{pTol}**, a reaction time of 1 h at room temperature under neat conditions. The catalyst exhibits full selectivity toward the anti-Markovnikov, i.e. linear, product, as shown by APT ^{13}C NMR after its isolation. Only a single signal containing the opposite phasing was observed in the aliphatic region of the ^{13}C NMR spectrum, corresponding to the single CH_3 group in the resulting product (Figure S8). Furthermore, analyses by ^1H NMR and GC–MS confirmed the presence of a single product isomer.

Analysis was performed by GC–MS and NMR for product characterization and GC for quantitative analysis. Besides remaining starting materials and formed product, three main side-products were observed. Ph_2SiH_2 was formed with a yield of 5 %, which is explained by a scrambling reaction of $PhSiH_3$ (Scheme 1). Besides GC and GC–MS analyses, Ph_2SiH_2 was also characterized using NMR techniques. The SiH_2 moiety gives rise to a distinctive peak in ^1H NMR at 5.04 ppm (J_{HSi} = 198 Hz) and in ^{29}Si NMR a peak was observed at –33.75 ppm, which were confirmed to belong to Ph_2SiH_2 by comparison to an authentic sample. Completing the stoichiometry in this reaction would result in the formation of one equivalent of SiH_4, which however could not be detected directly, presumably due to its high volatility (Scheme 2, top). To account for the incorporated silane in this by-product, it is assumed that the amount is equal to the amount of Ph_2SiH_2. This silane scrambling is a known side-reaction in hydrosilylation reactions[46–48] and it hampers product formation as it converts $PhSiH_3$ to less reactive side-products. A slight excess of 1.1 equivalents of $PhSiH_3$ was therefore used to maximize the yield of hydrosilylation reactions.

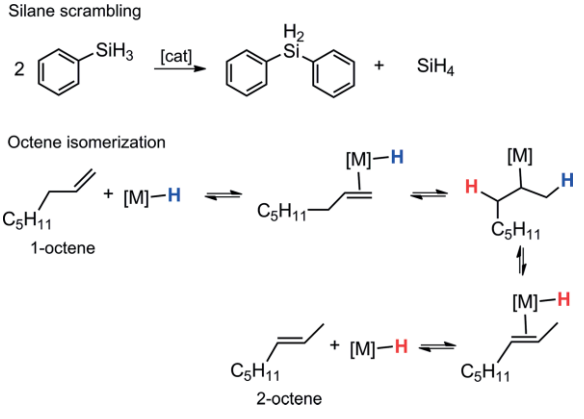

Scheme 2. Observed side-products and possible side-reaction pathways.

Furthermore, formation of octane (2 %) was observed, which can tentatively be explained by a reduction of the double bond, and formation of 2- and 3-octene (both 3 %). These latter products likely originate from isomerization of the carbon–carbon double bond of 1-octene, which may proceed via a separate catalytic cycle, catalyzed by **3^{pTol}**. A test reaction for the

Table 2. Hydrosilylation of 1-octene with $PhSiH_3$ with the cobalt complexes.[a]

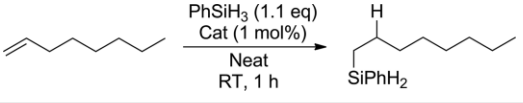

	Cat.	Conv. silane	Conv. alkene	Prod. yield	Isom. 1-oct	Octane	Ph_2SiH_2[b]
1	**3^{pTol}**	98	98	84	6	2	5
2	No cat	–	–	–	–	–	–
3	$CoCl_2$	16	4	–	–	–	–
4	$CoCl_2$ + PPh_3	95	3	–	3	Traces	–
5	**2^{pTol}**	60	42	32	4	1	–
6	**3^{Ph}**	99	98	75	5	2	3
7	**3^{Ph}** + THF	99	99	86	6	1	3

[a] All amounts are all given in percentage. Conversion is determined by GC (Supporting Information). [b] Amount of SiH_4 is considered equimolar to Ph_2SiH_2.

conditions of isomerization was performed. 1-Octene was mixed with 1 mol-% of $\mathbf{3}^{p\mathbf{Tol}}$ and stirred for 4 h at room temperature, which did not lead to any side-product formation. To proceed, the reaction likely needs a hydride source, i.e. $PhSiH_3$, to form the active Co–H catalyst (Scheme 2, bottom). The Co–H catalyzed reaction is assumed to follow a mechanism as proposed by Cramer in 1966,[49] in which the double bond of 1-octene initially coordinates in an η^2-fashion to Co, followed by addition of the hydride to C_α. Next, the hydride positioned at C_γ is added to Co, and the substrate dissociates from the metal resulting in 2-octene and the Co–H catalyst (Scheme 2).

With the benchmark hydrosilylation of 1-octene with phenylsilane established, a number of control experiments were performed to validate the need of the pre-catalyst. Experiments without the addition of a catalyst showed no conversion of the substrates and no product formation (Table 2, Entry 2). Using 1 mol-% of $CoCl_2$ as catalyst without addition of a co-ligand lead to low conversion of the substrates, i.e. 4 % conversion of 1-octene and 16 % conversion of phenylsilane, but no formation of the product was observed. Conversion of the substrates is attributed to ongoing heterogeneous processes (Table 2, Entry 3), as a result of the poor solubility of $CoCl_2$ in organic solvents. Addition of PPh_3 in combination with $CoCl_2$ again lead to low conversion of 1-octene (3 %), but high conversion of phenylsilane was obtained (95 %) (Table 2, Entry 4). The products of 1-octene conversion were analyzed as the isomerization (3 %) and hydrogenation (traces) products. The product of phenylsilane conversion was not identified, but it is likely that a minor fraction was used in the formation of hydride species, as these are needed for the 1-octene based side reactions (vide supra).

Comparison of Co^{II} complex $\mathbf{2}^{p\mathbf{Tol}}$ to Co^{I} complex $\mathbf{3}^{p\mathbf{Tol}}$ showed lower conversion of the substrates when using $\mathbf{2}^{p\mathbf{Tol}}$: 42 % for 1-octene and 60 % for phenylsilane with a lower selectivity toward octylphenylsilane, resulting in a yield of 32 % (Table 2, Entry 5). Low amounts of the 1-octene based side products were obtained and no silane scrambling was observed. The higher yield when using $\mathbf{3}^{p\mathbf{Tol}}$ could be explained by the reduced Co center, the η^2(CO)-coordination of the ligand, or a combination of these two. It is also plausible that the same active species is generated, albeit less efficiently, via reduction of the Co^{II} complex by the silane. Comparison of $\mathbf{3}^{p\mathbf{Tol}}$ to its phenyl substituted analogue $\mathbf{3}^{\mathbf{Ph}}$ showed a somewhat lower product yield of 75 % caused by lower solubility of $\mathbf{3}^{\mathbf{Ph}}$ as performing the reaction in THF resulted in 86 % yield (Table 2, Entry 6–7, respectively).

Substrate Scope

Extending the alkene substrate scope, allylbenzene was explored in a hydrosilylation reaction with $PhSiH_3$ catalyzed by $\mathbf{3}^{p\mathbf{Tol}}$. The reaction conditions were slightly changed to enhance product formation, to an extended reaction time of 4 h, and THF was used as the solvent instead of neat conditions, resulting in a 96 % conversion of allylbenzene, 97 % conversion of phenylsilane and a product yield of 84 %. Full selectivity toward the anti-Markovnikov product was obtained over the possible Markovnikov product formation (Table 3, Entry 1; Figure S9), and diphenylsilane was again obtained as a by-product (4 %). Styrene, however, resulted in a low yield of only 7 % (Table 3, Entry 2). Product determination by GC–MS, ^{1}H NMR, ^{13}C NMR and 2D ^{1}H-^{1}H COSY NMR (Figure S10–13), and subsequent quantitative analysis by GC showed the formation of both the Markovnikov and anti-Markovnikov product with respective yields of 3 % and 4 %. The formation of both products is more commonly observed when using styrene as the substrate.[10,50] The catalytic selectivity of styrene hydrosilylation with $\mathbf{3}^{p\mathbf{Tol}}$ was significantly lower than allylbenzene, with styrene conversion of 17 % and silane conversion of 31 % after 4 h. Besides silane scrambling, a number of unidentified by-products were observed in small quantities. Increasing the reaction time to 24 h did not improve the reaction significantly, as only the conversion improved poorly and larger amount of by-product diphenylsilane was obtained (Table 3, Entry 3).[51] Low conversion of styrene is presumably due to conjugation with the aromatic π-system, resulting in a less reactive C=C bond. The significantly higher product yield when using allylbenzene shows that the extra CH_2 group in the substrate makes for a great difference in reactivity, explained by the lesser extent of the conjugated π-system of allylbenzene.

The activity of $\mathbf{3}^{p\mathbf{Tol}}$ with a ketone was explored in the hydrosilylation of acetophenone, a substrate that is generally known to be more reactive due to the polarized nature of the carbon–oxygen double bond. The reaction of acetophenone with phenylsilane at room temp. for 4 h in THF catalyzed by

Table 3. Substrate scope of the hydrosilylation reactions with $\mathbf{3}^{p\mathbf{Tol}}$.[a]

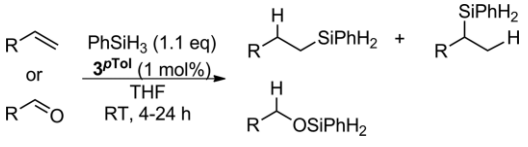

	Time	Substrate	Conv. silane	Conv. substrate	Prod. yield	Ph_2SiH_2[b]
1	4 h	Allylbenzene	97	96	84	4
2	4 h	Styrene	31	17	7 (3:4)[c]	5
3	24 h	Styrene	39	20	7 (3:4)[c]	7
4	4 h	Acetophenone	92	> 99	> 99[d]	4

[a] All amounts are all given in percentage. Conversion is determined by GC (see Supporting Information). [b] Amount of SiH_4 is considered equimolar to Ph_2SiH_2. [c] Markovnikov:anti-Markovnikov product, ratio determined by NMR and GC. [d] Analysis of 1-phenylethanol.

1 mol-% **3**^{pTol} leads to an excellent yield of the hydrosilylated product phenyl(1-phenylethoxy)silane (> 99 %) (Table 3, Entry 4). The product was quantified by GC and GC–MS analyses after acidification, forming the alcohol species 1-phenylethanol.

Chemoselectivity

Combining both an olefinic and ketone functionality in one substrate gives insight in possible chemoselectivity of the catalyst, for which the hydrosilylation of 5-hexen-2-one with $PhSiH_3$ was performed. After the reaction, an acidic workup was performed before analysis by GC. Addition of 2.1 equivalents of silane results in full conversion of both the olefin and ketone functionality after 24 h (Figure 4, product **C**), showing the catalysts capability of double addition on one substrate. Addition of a limiting amount of silane, i.e. 1 equivalent, is more indicative of the catalyst's behavior regarding chemoselectivity. After reaction for 4 h the substrates did not yet reach full conversion and GC analysis showed, next to 5-hexen-2-one and $PhSiH_3$, the three products of hydrosilylation (Figure 4) on a) the ketone, b) the olefin, c) both the ketone and olefin, in a 1:1:1 ratio, forming products **A**, **B** and **C**, respectively. Hence, the catalyst does not discriminate between a terminal olefin and a ketone under the chosen conditions, and the second addition seems to have a higher rate as this is obtained in similar ratio.

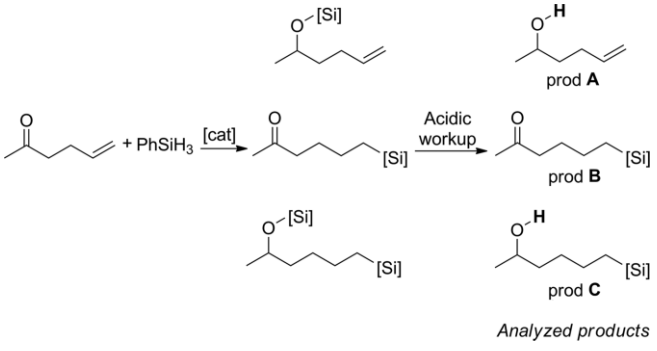

Figure 4. Products of the chemoselectivity experiment. Acidic workup was applied before analysis.

Discussion of the Mechanism

Cobalt-catalyzed hydrosilylation is a growing field with a number of highly efficient catalysts reported in recent years. The cobalt-catalyzed hydrosilylation reactions reported by Holland,[22] Huang[11] and Fout[24] (vide supra, Figure 1) are proposed to follow the Chalk–Harrod mechanism, in agreement with an in-depth investigation on mechanistic aspects, using a cobalt-bound phosphine substituted 2-iminopyridine ligand, as published by Rauchfuss, van Gastel and co-workers.[52] A rare example in which the specific role of a cooperative ligand is determined was shown by Peters and co-workers with a diphosphine-borane cobalt-dinitrogen complex (Figure 1, right), where the silane substrate is activated between the metal and the ligand backbone by addition of $–SiHPh_2$ to Co and insertion of the hydride into the Co–B bond.[34]

Investigations of the reaction of the cobalt precatalyst with phenylsilane suggest activation by formation of Co–H species, consistent with the Chalk–Harrod mechanism.[16] The role – if any – of the ketone moiety in cobalt catalysts presented herein cannot be established with certainty from the data at hand. Possible reactivity involving the ketone moiety include: a) hemilabile behavior upon changing the oxidation state of the metal center,[39] b) reversible addition of hydride to the moiety under catalytic conditions in analogy to the borane in Peters' catalyst, or c) its hydrosilylation to generate a catalytically active species. Recent experimental and computational investigations on similar ^{Ph}dpbp complexes with Co or Rh by Young and co-workers showed the ability of the ketone to reversibly accept a hydride equivalent to become an sp^3 hydroxyalkyl ligand.[42,53] Related processes are plausible under hydrosilylation conditions, but the exact nature of the involved species is unclear, and further investigations are ongoing to address details of the mechanism.

Conclusions

The investigated cobalt complexes equipped with a diphosphine-ketone ligand (^{R}dpbp) are active catalysts in hydrosilylation reactions with phenylsilane, showing the first example of catalysis with this family of complexes. Both, **2**^{pTol} and **3**^{pTol} are active in the hydrosilylation of 1-octene with phenylsilane, but **3**^{pTol} is superior. The Co^{I} catalyst proceeds under very mild conditions of 1 h, room temperature and without the need of a solvent, resulting in 84 % of octylphenylsilane. The scope of the alkene substrate was explored to a small extent, showing that the hydrosilylation of styrene leads to a low yield, whereas full conversion was reached using allylbenzene. The hydrosilylation of a polar double bond was shown to be the most facile reaction, with full substrate conversion and high selectivity for the product with > 99 % yield. The observed high catalytic reactivity combined with excellent product selectivity adds to the quickly developing field of cobalt-catalyzed hydrosilylation reactions.

Experimental Section

General Considerations: Unless stated otherwise, all reagents were purchased from commercial sources and used as received. Reactions are performed in a N_2-filled glovebox at room temperature with dry, degassed solvents. Deuterated benzene (C_6D_6) and deuterated dichloromethane (CD_2Cl_2) were degassed using the freeze-thaw-pump method (4 ×) and subsequently stored over molecular sieves. Dry diethylether, toluene and hexane were taken from an MB SPS-800 solvent purification set-up and degassed by bubbling N_2 through the solvent for 30 min and were further dried overnight over molecular sieves. CH_2Cl_2 was distilled from CaH_2 and tetrahydrofuran (THF) was distilled from sodium/benzophenone before use, both were degassed by bubbling N_2 through it for 30 min and stored over molecular sieves. THF, ether or petroleum ether (40–60 °C) used for column chromatography and calibration curve preparation were wet solvents of technical purity. Diphenylphosphine, $Pd(PPh_3)_4$, $CoCl_2$, metallic sodium and naphthalene were placed in the glovebox without additional purification. *o*-Bromoiodobenzene,

Et_3N and all substrates were degassed by bubbling N_2 for 30 min and dried with molecular sieves before use in the glovebox.

^1H, ^{13}C, ^{29}Si and ^{31}P NMR spectra (respectively 400, 100, 80 and 161 MHz) were recorded on an Agilent MRF400 or a Varian AS400 spectrometer at 25 °C. ^1H and ^{13}C NMR chemical shifts are reported in ppm relative to TMS using the residual solvent resonance as internal standard. ^{31}P NMR chemical shifts are externally referenced to 85 % aqueous H_3PO_4 and ^{29}Si NMR chemical shifts are externally referenced to TMS. Infrared spectra were recorded using a Perkin Elmer Spectrum One FT-IR spectrometer equipped with a N_2 flow over the crystal. UV-Vis spectra were measured using a Lambda 35 UV-Vis spectrometer. The UV-Vis samples were prepared under a N_2 atmosphere and sealed with a Teflon cap after which the spectra were recorded directly. ESI-MS spectra were recorded on a Walters LCT Premier XE KE317 Micromass Technologies spectrometer. Compounds of which elemental analysis is reported were either recrystallized or precipitated and dried under high vacuum overnight before submission and analysis was performed by the Mikroanalytisches Laboratorium Kolbe, Mülheim an der Ruhr, Germany. Gas chromatography mass spectrometry was carried out on a Perkin-Elmer Clarus 680 Gas Chromatograph with a PE Elite 5MS 15 m × 0.25 mm × 0.25 µm column, connected to a PerkinElmer Clarus SQ 8 T Mass Spectrometer. Gas chromatography was carried out on a PerkinElmer Clarus 500 Gas chromatograph with an Alltech EconocapTM ec TM 30.0 m × 0.32 mm ID × 0.25 µm, 5 % phenyl and 95 % methylpolysiloxane column. In general method 1 was used: 50 °C for 3 min, 40 °C/min increase for 5.75 min to reach 280 °C, 280 °C for 3 min (total 11.75 min). For analysis of reactions using 5-hexen-2-one, method 2 was used: 50 °C for 3 min, 5 °C/min increase for 46 min to reach 280 °C, 280 °C for 3 min (total 52 min). Details on X-ray crystal structure determination and selected spectra are given in the Supporting Information.

CCDC 1871266 (for **2$^{p\text{Tol}}$**) contains the supplementary crystallographic data for this paper. These data can be obtained free of charge from The Cambridge Crystallographic Data Centre.

Synthesis

o-Bromophenyl-di-*p*-tolylphosphine[39,54]

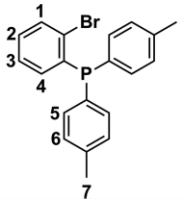

o-Bromo-iodobenzene (6 mL, 46.7 mmol) was dissolved in toluene (10 mL) in a Schlenk tube under N_2 atmosphere. In consecutive order, a mixture of di-*p*-tolylphosphine (10.1 g, 46.7 mmol) in toluene (15 mL), dry Et_3N (10 mL, 70.1 mmol) and $Pd(PPh_3)_4$ (296 mg, 0.26 mmol) in toluene (20 mL) were added resulting in a yellow solution. The mixture was heated to 80 °C for 12 h, after which the deep brown mixture was washed with brine (2 × 65 mL). The aqueous phase was extracted with Et_2O (2 × 75 mL, 4 × 35 mL). The combined organic layers were dried with $MgSO_4$, filtered and the solvent was evaporated. Cold MeOH (3 × 15 mL) was used to wash the crude product. The product was dried in vacuo and isolated as an off-white powder (14.7 g, 39.7 mmol, 85 %). ^1H NMR (C_6D_6): δ_H = 7.34 (ddd, $^3J_{HH}$ = 7.9, $^3J_{HP}$ = 3.6 Hz, $^4J_{HH}$ = 1.2 Hz, 1H, *H4*), 7.29 (t, $^3J_{HH}$ = 7.8 Hz, $^3J_{HP}$ = 7.8 Hz, $^4J_{HH}$ = 1.7 Hz, 4H, *H5*), 6.93 (dt, $^3J_{HH}$ = 7.7 Hz, $^3J_{HP}$ 2.1 Hz, $^4J_{HH}$ = 2.1 Hz, 1H, *H1*), 6.87 (d, $^3J_{HH}$ = 7.7 Hz, 4H, *H6*), 6.76 (td, $^3J_{HH}$ = 7.5 Hz, $^4J_{HH}$ = 1.2 Hz, 1H, *H3*), 6.64 (td, $^3J_{HH}$ = 7.7 Hz, $^4J_{HH}$ = 1.7 Hz, 1H, *H2*), 1.97 (s, 6H, *7*). ^{13}C NMR (C_6D_6): δ_C = 138.61, 134.43, 134.25, 134.05, 132.94 (d, *J* = 2.2 Hz), 129.69, 129.48, 129.41, 127.05, 20.78. ^{31}P NMR (C_6D_6): δ_P = –6.31.

$^{p\text{Tol}}$dpbp (1$^{p\text{Tol}}$)[39]

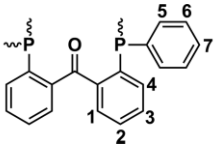

o-Bromophenyl-di-*p*-tolyl-phosphine (4.93 g, 13.4 mmol) was suspended in Et_2O (30 mL). The light-yellow suspension was cooled to –50 °C using an acetone dry ice bath. *n*BuLi (1.6 M in hexane, 16 mmol, 10 mL) was added drop wise while stirring, resulting in a rapid color change form yellow to brown. Within 30 min, the reaction mixture was warmed up to room temperature and was directly cooled down again to –50 °C, after which a solution of *N*,*N*-dimethylcarbamoylchloride (0.61 mL, 6.5 mmol) in Et_2O (15 mL) was added drop wise over 20 minutes. During addition, the temperature of the bath was kept between –35 °C and –45 °C, after which the suspension was stirred overnight allowing the mixture to warm up to room temperature. The reaction was cooled down again and treated at 0 °C with a degassed 2.5 M NH_4Cl solution in water (38 mL, 4.5 g, 85 mmol NH_4Cl) turning the suspension orange-yellow. The product was extracted with Et_2O and dried with $MgSO_4$ and solvents were evaporated. The obtained yellow compound was washed with MeOH, resulting in the product as a yellow powder after solvent removal (2.41 g, 4.0 mmol, 61 %). ^1H NMR (C_6D_6): δ_H = 7.37 (t, *J* = 7.6 Hz, 8H, *H5*), 7.37 (m, 2H, *H4*), 7.31 (dd, *J* = 7.7, 2.4 Hz, 2H, *H1*), 6.95 (td, *J* = 7.5, 1.1 Hz, 2H, *H2/3*), 6.91 (d, *J* = 7.7 Hz, 8H, *H6*), 6.83 (td, *J* = 7.5, 1 Hz, 2H, *H3/2*), 2.03 (s, 12H, *H7*). ^{13}C NMR ($CDCl_3$): δ_C = 197.35 (t, *J* = 3 Hz, *C*=O), 144.64 (dd, *J* = 24.4, 1 Hz, Cq^{Ar}), 140.68 (*J* = 26.1, 2.2 Hz, Cq^{Ar}), 138.21 (Cq^{Ar}), 135.56 (dt, *J* = 3, 11 Hz, Cq^{Ar}), 135.00 (CH^{Ar}), 134.45 (m, CH^{Ar}), 131.03 (t, *J* = 3.3 Hz, CH^{Ar}), 130.66 (CH^{Ar}), 129.48 (m, CH^{Ar}), 128.00 (CH^{Ar}), 21.21 (–CH_3). ^{31}P NMR (C_6D_6): δ_P = –9.77. ATR-IR $\tilde{\nu}$: 3012, 2956, 2920, 2863, 1910, 1738, 1664, 1598, 1495, 1446, 1395, 1296, 1271, 1243, 1185, 1090, 1018, 928, 805, 747, 637, 507 cm^{-1}. ESI-MS (MeCN $AgNO_3/H_2O$) *m/z*: $[2M + Ag]^+$: 1319.3529, calc: 1319.3534. Elemental analysis: calcd: C 81.17, H 5.98, found C 80.84, H 6.05.

($^{p\text{Tol}}$dpbp)$CoCl_2$ (2$^{p\text{Tol}}$): $^{p\text{Tol}}$dpbp (101.0 mg, 0.17 mmol) and $CoCl_2$ (65.0 mg, 0.16 mmol) were suspended in CH_2Cl_2 (5 mL) and stirred for 17 h, resulting in a green solution. The product was precipitated from CH_2Cl_2/hexane, collected via filtration, extracted using CH_2Cl_2 and dried in vacuo resulting in a green powder (88.2 mg, 0.12 mmol, 72 %). ^1H NMR (CD_2Cl_2): δ_H = 18.82, 13.63, 11.77, 9.99, 7.88, 0.54, 0.10, –0.55. ATR-IR $\tilde{\nu}$: 1634, 1499, 1286, 1096, 805. Solution cell IR (THF, cm^{-1}): 1662, 1598 (weak) cm^{-1}. ESI-MS *m/z*: $[M - Cl]^+$ obs. 700.1297, calcd. 700.1262. UV-Vis (CH_2Cl_2) λ_{max}, nm: 603, 650, 734, 760. Elemental Analysis: calcd: C 66.02, H 5.42, found C 66.86, H 4.93.

($^{p\text{Tol}}$dpbp)CoCl (3$^{p\text{Tol}}$):[39] Naphthalene (79.9 mg, 0.62 mmol) was dissolved in THF (4 mL). A lump of Na^0 was added and the mixture was stirred for 3 h, after which a dark green solution was obtained. $CoCl_2$ (65.0 mg, 0.50 mmol) and $^{p\text{Tol}}$dpbp (300.6 mg, 0.49 mmol) were suspended in THF (25 mL) and cooled to –78 °C. The naphthalide solution was filtered and added to the cooled cobalt mixture. This final mixture was stirred further for 1 h at –78 °C and for 18 h at room temperature, after which it was concentrated in vacuo to ≈ 1.5 mL. Hexane was added (5 mL) and the precipitated solids were collected by filtration. The product was extracted with THF

and dried in vacuo, resulting in (^{pTol}dpbp)CoCl as a brown powder with a yield of 86 % (300.3 mg, 0.43 mmol). ^{1}H NMR (C_6D_6): δ_H = 31.59, 20.00, 17.64 (s, 3H, –*Me*), 14.34, 13.54, 9.21 (s, 3H, –*Me*), –0.06, –0.98 (broad), –6.07, –7.97, –16.38. ATR-IR $\tilde{\nu}$: 2919, 2863, 1599, 1498, 1434, 1397, 1258, 1241, 1189, 1096, 1019, 917, 803, 777, 693, 626, 510 cm^{-1}. UV-Vis: λ_{max}: 525 nm. Elemental analysis: calcd: C 70.24, H 5.18, found C 70.00, H 5.37.

Catalysis

All catalytic reactions were performed *in duplo* and given values are the average of the two runs, unless stated otherwise. Conversion and yield were determined by GC analysis, for which calibration curved were prepared for all substrates and products. The yields of product arising from 1-octene isomerization were determined using the calibration curve for 1-octene. Next to the characterized and quantified products, a number of small signals (GC area > 1 %) were generally obtained in GC analysis. These products could not be identified; they are therefore not described in the analysis. Further analysis and characterizations are described in the Supporting Information.

Hydrosilylation Method 1 (1-Octene): In a glovebox, catalyst (0.01 mmol) was added to a 6 mL vial. 1-Octene (0.160 mL, 1.0 mmol) was added. Addition of $PhSiH_3$ (0.135 mL, 1.1 mmol) while stirring caused bubbling of the mixture and resulted in a clear brown solution after 1 minute. The solution was stirred for 1 h at room temperature and then taken out of the glovebox, where it was opened in air. The mixture was filtered through a plug of silica (≈ 1 cm) using THF as eluent (total amount of mixture: 25 mL) to remove cobalt. From this a GC–MS sample was taken. For GC analysis, 1 mL of the prepared solution was added to 2.5 mL of a mesitylene (Mes) solution (internal standard, 0.017 M Mes solution: 102.4 mg of Mes in 50 mL of THF) and THF was added to a total volume of 10 mL.

Hydrosilylation Method 2 (Allylbenzene and Styrene): In a glovebox, **3^{pTol}** (7.0 mg, 0.01 mmol) was dissolved in THF (1 mL) resulting in a clear brown solution. A mixture of two substrates was added with a syringe while stirring. The solution was stirred for 4 h at room temperature and then taken out of the glovebox and opened in air. The mixture was filtered through a silica plug (≈ 1 cm) using THF as eluent (total amount of mixture: 25 mL) to remove cobalt. From this a GC–MS sample was taken. For GC analysis, 1 mL of the prepared solution was added to 2.5 mL of a mesitylene (Mes) solution (internal standard, 0.017 M Mes solution: 102.4 mg of Mes in 50 mL of THF) and THF was added to a total volume of 10 mL.

Hydrosilylation Method 3 (Acetophenone and 5-Hexen-2-one): In a glovebox, **3^{pTol}** (7.0 mg, 0.01 mmol) was added to a small vial and dissolved in THF (1 mL) resulting in a clear brown solution. A mixture of two substrates was added with a syringe while stirring. The solution was stirred for 4 h at room temperature and taken out of the glovebox and opened in air. The reaction mixture was transferred to a separation funnel using Et_2O and quenched with a HCl solution (2.5 mL, 10 %) to form the alcohol product. The aqueous layer was removed, and the organic layer was washed with H_2O (0.2 mL). The aqueous layer was washed Et_2O (3 × 2 mL). The Et_2O fractions were filtered through a silica plug (≈ 1 cm, total volume after Et_2O addition: 25 mL). For GC analysis, 1 mL of the prepared solution was added to 2.5 mL of a mesitylene (Mes) solution (internal standard, 0.017 M Mes solution: 102.4 mg of Mes in 50 mL of THF) and THF was added to a total volume of 10 mL. For NMR analysis, the solvent and precursors were evaporated in vacuo resulting in a turbid white liquid.

Isolation of Octylphenylsilane: In a nitrogen-filled glovebox, **3^{pTol}** (21.0 mg, 0.03 mmol) was dissolved in THF (1 mL). 1-Octene (0.470 mL, 3.0 mmol) and $PhSiH_3$ (0.405 mL, 3.3 mmol) were subsequently added, and bubbling occurred upon addition of the latter. The clear brown solution was stirred for 4 h and taken out of the glovebox. Air was bubbled through the solution for 20 min to quench the catalyst, turning the solution green. Cobalt was removed by filtration through a silica plug (≈ 1 cm) with petroleum ether. The product was isolated by column chromatography using petroleum ether as the eluent. Evaporation of the solvents in vacuo resulted in a turbid white liquid (319 mg, 1.45 mmol, 48 %). ^{1}H NMR (C_6D_6): δ = 7.52–7.43 (m, 3H, Ar–H), 7.18–7.01 (m, 2H, Ar–H), 4.48 (t, $^3J_{HH}$ = 3.7 Hz, $^2J_{HSi}$ = 190.99 Hz, 2H, Si–H_2), 1.47–1.37 (m, 2H, –CH_2), 1.33–1.13 (m, 10H, –CH_2), 0.94–0.87 (t, $^3J_{HH}$ = 6.9 Hz, 3H, –CH_3), 0.87–0.79 (m, 2H, –CH_2). ^{13}C NMR (C_6D_6): δ = 135.6 (Ar–CH), 132.9 (Ar–CH), 129.9 (Ar–CH), 128.4 (Ar–CH), 33.3 (octyl), 32.3 (octyl), 29.6 (octyl), 25.5 (octyl), 23.1 (octyl), 14.4 (–CH_3), 10.4 (SiH_2–CH_2). INEPT ^{29}Si-NMR (C_6D_6): δ –31.0. GC–MS: Octylphenylsilane: *t*: 15.9, *m/z*: [M – C_6H_6]$^+$ obs. 142.2, calcd: 142.1. GC: Octylphenylsilane *t*: 3.6.

Silane Activation: In a glovebox, **3^{pTol}** (21.0 mg, 0.03 mmol) was dissolved in C_6D_6 (0.4 mL) and stirred. $PhSiH_3$ (15.6 mg, 0.14 mmol) was added to a second vial and diluted with C_6D_6 (1 mL). 0.6 mL of the $PhSiH_3$ solution (0.09 mmol) was added to the solution of **3^{pTol}** and the mixture was stirred for 15 min, after which it was filtered into a Young-type NMR tube. ^{1}H NMR (C_6D_6): δ –11.98 (m, hydride), ^{31}P NMR (C_6D_6): δ_P broad signals: 74, 70, 64, 60. Sharp signals: –16.1, –16.2, –16.4, –17.3, –17.6. Spectra are shown in the Supporting Information, Figure S14 and S15.

Acknowledgments

D. V. and M. E. M. would like to thank the Sectorplan Natuuren Scheikunde (Tenure-track grant at Utrecht University) for financial support. The X-ray diffractometer was financed by The Netherlands Organization for Scientific Research (NWO).

Keywords: Silane chemistry · Cobalt · Hydrosilylation · Homogeneous catalysis · Cooperative catalysis

[1] J. Sun, L. Deng, *ACS Catal.* **2016**, *6*, 290–300.
[2] X. Du, Z. Huang, *ACS Catal.* **2017**, *7*, 1227–1243.
[3] J. V. Obligacion, P. J. Chirik, *Nat. Rev.* **2018**, *2*, 15–34.
[4] K. Junge, V. Papa, M. Beller, *Chem. Eur. J.* **2019**, *25*, 122–143.
[5] R. J. Hofmann, M. Vlatkovic, F. Wiesbrock, *Polymer* **2017**, *9*, 534.
[6] J. L. Speier, J. A. Webster, G. H. Barnes, *J. Am. Chem. Soc.* **1957**, *79*, 974–979.
[7] B. D. Karstedt, General Electric Company., U. S. Patent US3775452A, **1973**.
[8] T. K. Meister, K. Riener, P. Gigler, J. Stohrer, W. A. Herrmann, F. E. Kühn, *ACS Catal.* **2016**, *6*, 1274–1284.
[9] R. Langer, Y. Diskin-Posner, G. Leitnus, L. J. W. Shimon, Y. Ben-David, D. Milstein, *Angew. Chem. Int. Ed.* **2011**, *50*, 9948–9952; *Angew. Chem.* **2011**, *123*, 10122.
[10] A. M. Tondreau, C. C. H. Atienza, K. J. Weller, S. A. Nye, K. M. Lewis, J. G. P. Delis, P. J. Chirik, *Science* **2012**, *335*, 567–570.
[11] X. Du, Y. Zhang, D. Peng, Z. Huang, *Angew. Chem. Int. Ed.* **2016**, *55*, 6671–6675; *Angew. Chem.* **2016**, *128*, 6783.
[12] T. J. Steiman, C. J. Uyeda, *J. Am. Chem. Soc.* **2015**, *137*, 2081–2084.
[13] I. Buslov, J. Becouse, S. Mazza, M. Montandon-Clerc, X. Hu, *Angew. Chem. Int. Ed.* **2015**, *54*, 14523–14526; *Angew. Chem.* **2015**, *127*, 14731.
[14] I. Buslov, S. C. Keller, X. Hu, *Org. Lett.* **2016**, *18*, 1928–1931.
[15] I. Pappas, S. Treacy, P. J. Chirik, *ACS Catal.* **2016**, *6*, 12295–12299.
[16] A. J. Chalk, J. F. Harrod, *J. Am. Chem. Soc.* **1965**, *87*, 1133–1135.
[17] M. A. Schroeder, M. A. Wrighton, *J. Organomet. Chem.* **1977**, *128*, 345–358.

[18] S. Sakaki, N. Mizoe, M. Sugimoto, *Organometallics* **1998**, *17*, 2510–2523.
[19] A. K. Roy, R. B. Taylor, *J. Am. Chem. Soc.* **2002**, *124*, 9510–9524.
[20] M. Brookhart, B. E. Grant, *J. Am. Chem. Soc.* **1993**, *115*, 2151–2156.
[21] Z. Mo, Y. Liu, L. Deng, *Angew. Chem. Int. Ed.* **2013**, *52*, 10845–10849; *Angew. Chem.* **2013**, *125*, 11045.
[22] C. Chen, M. B. Hecht, A. Kavara, W. W. Brennessel, B. Q. Mercado, D. J. Weix, P. L. Holland, *J. Am. Chem. Soc.* **2015**, *137*, 13244–13247.
[23] C. H. Schuster, T. Diao, I. Pappas, P. J. Chirik, *ACS Catal.* **2016**, *6*, 2632–2636.
[24] A. D. Ibrahim, S. W. Entsminger, L. Zhu, A. R. Fout, *ACS Catal.* **2016**, *6*, 3589–3593.
[25] D. Noda, A. Tahara, Y. Sunada, H. Nagashima, *J. Am. Chem. Soc.* **2016**, *138*, 2480–2483.
[26] A. Gorczynski, M. Zaranek, S. Witomska, A. Bocian, A. R. Stefankiewicz, M. Kubicki, V. Patroniak, P. Pawluc, *Catal. Commun.* **2016**, *78*, 71–74.
[27] Y. Gao, L. Wang, L. Deng, *ACS Catal.* **2018**, *8*, 9637–9646.
[28] A. Sanagawa, H. Nagashima, *Organometallics* **2018**, *37*, 2859–2871.
[29] J. Guo, X. Shen, Z. Lu, *Angew. Chem. Int. Ed.* **2017**, *56*, 615–618; *Angew. Chem.* **2017**, *129*, 630.
[30] L. Yong, K. Kirleis, H. Butenschon, *Adv. Synth. Catal.* **2006**, *348*, 833–836.
[31] Z. Mo, J. Xiao, Y. Gao, L. Deng, *J. Am. Chem. Soc.* **2014**, *136*, 17414–17417.
[32] C. Wu, W. J. Teo, S. Ge, *ACS Catal.* **2018**, *8*, 5896–5900.
[33] H. Wen, X. Wan, Z. Huang, *Angew. Chem. Int. Ed.* **2018**, *57*, 6319–6323; *Angew. Chem.* **2018**, *130*, 6427–6431.
[34] M. A. Nesbit, D. J. M. Suess, J. C. Peters, *Organometallics* **2015**, *34*, 4741–4752.
[35] Y. Li, J. A. Krause, H. Guan, *Organometallics* **2018**, *37*, 2147–2158.
[36] a) T. Dombray, C. Helleu, C. Darcel, J.-B. Sortais, *Adv. Synth. Catal.* **2013**, *355*, 3358–3362; b) D. Bézier, G. T. Venkanna, L. C. Misal Castro, J. Zheng, T. Roisnel, J.-B. Sortais, C. Darcela, *Adv. Synth. Catal.* **2012**, *354*, 1879–1884.
[37] Y. Liu, L. Deng, *J. Am. Chem. Soc.* **2017**, *139*, 1798–1801.
[38] a) C. Wang, W. J. Teo, S. Ge, *ACS Catal.* **2017**, *7*, 855–863; b) W. J. Teo, C. Wang, Y. W. Tan, S. Ge, *Angew. Chem. Int. Ed.* **2017**, *56*, 4328–4332; *Angew. Chem.* **2017**, *129*, 4392; c) C. Wang, W. J. Teo, S. Ge, *Nat. Commun.* **2017**, *8*, https://doi.org/10.1038/s41467-017-02382-7; d) H. L. Sang, S. Yu, S. Ge, *Chem. Sci.* **2018**, *9*, 973–978.
[39] D. G. A. Verhoeven, M. A. C. van Wiggen, J. Kwakernaak, M. Lutz, R. J. M. Klein Gebbink, M.-E. Moret, *Chem. Eur. J.* **2018**, *24*, 5163–5172.
[40] D. G. A. Verhoeven, M.-E. Moret, *Dalton Trans.* **2016**, *45*, 15762–15778.
[41] B. W. H. Saes, D. G. A. Verhoeven, M. Lutz, R. J. M. Klein Gebbink, M.-E. Moret, *Organometallics* **2015**, *34*, 2710–2713.
[42] Related reactivity: S. Sung, Q. Wang, T. Krämer, R. D. Young, *Chem. Sci.* **2018**, *9*, 8234–8241.
[43] The ^{31}P NMR shows a few very weak signals around –15 ppm, which are attributed to ligand decomposition, and broad features around 45 and 60 ppm.
[44] a) S. P. Semproni, C. Milsmann, P. J. Chirik, *J. Am. Chem. Soc.* **2014**, *136*, 9211–9224; b) M. L. Scheuermann, S. P. Semproni, I. Pappas, P. J. Chirik, *Inorg. Chem.* **2014**, *53*, 9463–9465.
[45] Hydrosilylation of 1-octene using diphenylsilane, triethoxysilane or dimethylphenylsilane resulted in low product yields and increased amounts of side products as determined by GC–MS.
[46] Y. Nakajima, S. Shimada, *RSC Adv.* **2015**, *5*, 20603–20616.
[47] M. Itoh, K. Inoue, J. I. Ishikawa, K. Iwata, *J. Organomet. Chem.* **2001**, *629*, 1–6.
[48] B. Becker, R. J. P. Corriu, C. Guerin, B. J. L. Henner, *J. Organomet. Chem.* **1989**, *369*, 147–154.
[49] a) T. C. Morrill, C. A. D'Souza, *Organometallics* **2003**, *22*, 1626–1629; b) R. Cramer, *J. Am. Chem. Soc.* **1966**, *88*, 2272–2282; c) T. J. Mooibroek, E. C. M. Wenker, W. Smit, I. Mutikainen, M. Lutz, E. Bouwman, *Inorg. Chem.* **2013**, *52*, 8190–8201.
[50] J. W. Sprengers, M. de Greef, M. A. Duin, C. J. Elsevier, *Eur. J. Inorg. Chem.* **2003**, 3811–3819.
[51] Increasing the reaction temperature to 60 °C did not result in an improvement of the yield.
[52] W.-Y. Chu, R. Gilbert-Wilson, T. B. Rauchfuss, M. van Gastel, F. Neese, *Organometallics* **2016**, *35*, 2900–2914.
[53] S. Sung, J. Kang Boon, J. J. C. Lee, N. A. Rajabi, S. A. Macgregor, T. Kramer, R. D. Young, *Organometallics* **2017**, *36*, 1609–1617.
[54] Q. Shen, J. F. Hartwig, *J. Am. Chem. Soc.* **2007**, *129*, 7734–7735.

Received: October 8, 2018